# Hierarchical Porous $TiO_2$ thin films by soft and dual templating. A quantitative approach of specific surface and porosity.

Catherine Henrist[a,b], Jennifer Dewalque[a], Rudi Cloots[a,b], Bénédicte Vertruyen[a], Jonathan Jonlet[a], Pierre Colson[a]

[a]University of Liege, Department of Chemistry, GREENMAT-LCIS, B6 Sart Tilman, 4000 Liege, Belgium

[b]University of Liege, Center for Applied Technology in Microscopy (CATμ), B6 Sart Tilman, 4000 Liege, Belgium

**Abstract**

Hierarchical porous structures, with different pore sizes, including pores larger than 10 nm, constitute an important field of research for many applications such as selective molecule detection, catalysis, dye-sensitized solar cells, nanobiotechnology and nanomedecine. However, increasing the pore size logically results in the decrease of specific surface. There is a need to quantify and predict the resulting porosity and specific surface.

We have prepared hierarchical porous $TiO_2$ thin films either by surfactant templating (soft) or dual surfactant/nanospheres templating (soft/hard). They all show narrow, bimodal distribution of pores.

Soft templating route uses a modified sol-gel procedure by adding a swelling agent (polypropylene glycol) to a precursor solution containing Ti alkoxide and block-copolymer surfactant. This scheme leads to very thin films showing high specific surface and bimodal porosity with diameters of 10 nm and 54 nm.

Dual templating route combines a precursor solution made of Ti alkoxide and block-copolymer surfactant with polystyrene (PS) nanospheres (diam. 250 nm) in a one-pot simple process. This gives thicker films with a bimodal distribution of pores (8 nm and 165-200 nm). The introduction of PS nanospheres in the surfactant-Ti system does not interfere with the soft templating process and results in a macroporosity with a pore diameter 20-30% smaller than the original beads diameter.

The dye loading of hierarchical films is compared to pure surfactant-templated $TiO_2$ films and shows a relative decrease of 29% for soft templating and 43% for dual templating.

The microstructure of bimodal porous films is characterized by several techniques such as transmission and scanning electron microscopy, X-ray diffraction, profilometry and ellipsometry. Finally, a geometrical model is proposed and validated for each system, based on the agreement between calculated specific surfaces and experimental dye loading with N719 dye.

## 1. Introduction

Porous $TiO_2$ thin films are extensively studied due to their widespread fields of applications, mainly in photovoltaics [1] and photocatalysis [2] but also in gas sensing [3] and water splitting [4].

Doctor-blade method and screen printing are currently the most frequently used techniques to produce porous $TiO_2$ thin films for applications in dye-sensitized solar cells (DSSC). The influence of tortuous and narrowed pore channels on the diffusion rate of large molecules is negative and limit the infiltration of dye, redox species and organic hole conductors required to assemble solar cells. The porosity size and shape in randomly packed nanoparticles is defined by the interstices between neighboring particles and is limited by particles diameter.

Bimodal macro-mesoporous materials have attracted increasing interest due to their improved textural properties and potential applications[5]. Amphiphilic block-copolymers, among them the mostly used Pluronic surfactants, are generally used as soft templates to generate ordered mesoporosity in the films, following an evaporation-induced self assembly (EISA) or micelles packing (EIMP) mechanisms[6,7]. This synthesis route gives excellent regularity and monodispersity of pores network but is limited to pore size below 10 nm[8]. Swelling of the micelles by a suitable pore expander, which is selectively soluble in the core of the micelle, is an attractive route for the preparation of larger pores derived from EISA/EIMP methods. However, the introduction of a third (and sometimes fourth) component to the surfactant/Ti pair gives rise to complex multiphases or demixing systems that are not easy to control[9,10].

Besides, latex or silica nanospheres can be employed as hard-templates to build inverse-opal structures which are a macroporous replica of the hexagonal packing of spheres[11 -14], giving access to ordered porosity of any size, determined by the diameter of nanobeads. However, porous structures with macropores are characterized by a lower specific surface than mesoporous systems, which limits their interfacial reactivity and adsorption capabilities. For this reason, the combination of macro- and mesopores constitutes a very attractive strategy to produce thin films with highly structured interface, high specific surface, accessible and ordered pores as well as facilitated entry of viscous or hindered chemical species.

Latex beads based on polymethylmethacrylate (PMMA) polymer have been used as colloidal template in combination with block-copolymers acting as soft templates[15], in an attempt to introduce a large scale roughness for better light scattering in DSSCs, either in a one-pot route or as a top-layer. However the PMMA microbeads (diam. 1 μm) showed to be badly

dispersed leading to a heterogeneous film, thinner than the diameter of a single bead and exhibiting a lot of cracks. Zhao et al.[16] have used polystyrene (PS) microspheres and block-copolymer surfactant in sequential steps, infiltrating the surfactant/Ti precursor into the microspheres packing for photocatalysis application. While quite often reported [5,17-19], the template-infiltration two-step process is time consuming. Qi et al.[20] have shown that a one-pot route based on the self-assembly of PS spheres in the presence of $TiO_2$ sol-gel precursor can give regular and crack-free films with a macroporosity slightly smaller than the beads diameter.

Since most applications of bimodal porous thin films of Anatase rely on the interface between the porous semiconductor and an adsorbed molecule (pollutant to be degraded, dye for sensitizing, gas to be detected, electrolyte for regeneration, water to be split, ..), it is important to control and even predict the overall percentage of porosity and specific surface obtained when two pore sizes are combined in a single film.

This paper reports the preparation of bimodal porous $TiO_2$ films by a soft-templating route (ST) or a dual-templating route (DT). The films are extensively described in terms of thickness, pore sizes, crystal size and specific surface. A geometrical model is proposed to describe the porous structure obtained after a soft-templating or a dual-templating process, allowing to predict by simple calculation the specific surface and percentage of air in any bimodal porous material, based on spatial organization of pores, crystal size and wall thickness.

## 2. Experimental details

### 2.1 Soft Templating route (ST)

The procedure was adapted from Malfatti et al.[8] with some modifications aiming at increasing the film thickness obtained by dip-coating.

We prepared the soft-templated films from a precursor solution containing $TiCl_4$, n-butanol, water, polypropylene glycol (PPG, Mn = 4000) and Pluronic block-copolymer surfactant (F127 , $PEO_{106}$-$PPO_{70}$-$PEO_{106}$, Sigma Aldrich) in molar ratio 1:40:10:0.00625: 0.004. Tetrahydrofuran (THF,VWR, 29 vol% of the final solution) is added to help the dissolution of PPG. This composition was selected from[8] in order to generate a quite narrow population of large mesopores of approximately 40 nm, in addition to the small mesopores commonly observed from F127 templating. The solution is stirred at room temperature for 3h allowing micellization.

7.2 ml of n-butanol and 0.2 g of F127 were added in a flask with 440 µl of $TiCl_4$. The solution was stirred for 5 min until all the F127 was dissolved. Then 720 µl of water and 0.9 g of PPG (Mn = 4000) were added into the solution. Finally, $V_{THF}$ was added to the solution. $V_{THF}$ is defined as the percentage volume of THF relative to the final solution and we used $V_{THF}$ = 29 % .

We used the dip-coating technique to deposit the films onto silicon wafers (MEMC, Electronic Materials, it). To ensure good wetting of the solution, the substrates are previously passivated ($HNO_3$ 1M, 24 h) and thoroughly wiped with tissue soaked in ethanol then with a tissue soaked in acetone. The substrates are then dipped from the precursor solution under controlled humidity of 20% at a withdrawal speed of 2 mm/s. The films are stabilized during 15 minutes on a hot plate preheated at 300°C. Finally, we apply a calcination step in an oven with a ramp of 1°C/min up to 360°C and keep the sample at this temperature for 10 to 120 minutes. The films are allowed to cool down in the oven before analysis.

### 2.2 Dual Templating Route (DT)

Two templates are combined in a mixed precursor solution: the widely studied Pluronic block-copolymer P123 ($PEO_{20}$-$PPO_{70}$-$PEO_{20}$) and polystyrene (PS) nanospheres (Bangs Laboratories, Inc.) with diameter 250 nm. The nanospheres aqueous suspension (10 wt%) requires a pre-treatment to avoid uncontrolled hydrolysis of Ti isopropoxide promoted by water when mixed with the sol-gel precursor solution. The flowchart of solutions and suspension processing is depicted in Figure 1.

Water from the commercial nanospheres suspensions has to be eliminated. Large size nanospheres (250 nm) are easily centrifugated and can be obtained as nearly "dry" spheres.

Sol-gel precursor solution was prepared by mixing a solution of P123 (1.005 g) in n-butanol (11.2 ml) with a solution of titanium (IV) isopropoxide (3.96 g) in concentrated HCl (2.07 mL). The final sol-gel precursor solution has a molar ratio of 1 Ti: 0.0124 P123:1.78 HCl: 8.7 n-butanol. The solution is stirred for 3h to allow micellization.

The nanospheres are added to the sol-gel precursor to reach a final proportion of ~9 vol%.

50 µL of the resulting mixed precursor solution is deposited by spin coating on passivated silicon substrates: 2 s at 1930 rpm, 2 s at 2500 rpm and finally 30 s at 6900 rpm. The films are then calcinated during 30 min at 500°C under oxygen flow (heating rate: 500°C/h).

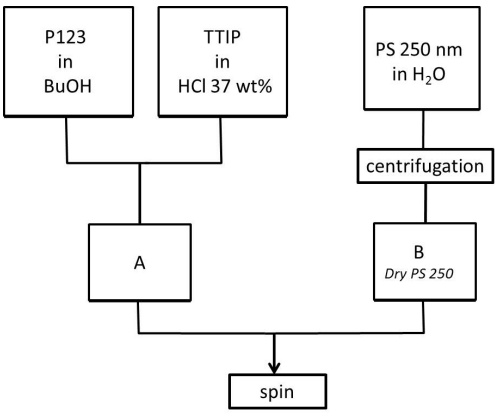


**Figure 1. Flowchart of dual templating route. TTIP stands for Ti isopropoxide**

### 2.3 Characterization

We used scanning electron microscopy (SEM) to visualize the microstructure of the films. The samples were sputtered with gold before being observed at 15 kV in a FEG-SEM (XL30, FEI).

The porosity of films has been checked by transmission electron microscopy (TEM) on a Tecnai G2 TWIN (FEI) working at 200 kV. Before imaging, the films were scratched from the substrate and sonicated in a few drops of ethanol. A drop of suspension was then deposited on a carbon-coated copper grid.

Pore size and wall thickness has been evaluated by image analysis from SEM and TEM micrographs.

Percentage of pores in the film is calculated from the refractive index determined with a spectroscopic ellipsometer (GES5E, Sopralab) using Effective Medium approximation [21].

X-ray Diffractometry (XRD) was performed on a D8 diffractometer (Bruker) working in grazing incidence (CuK$\alpha$, incidence angle 2°, stepsize 0.04°, scan rate 6 sec/step). We

identified the crystallization of Anatase $TiO_2$ by observing the appearance of 101 diffraction peak (25,36 °2θ). This peak is also used to calculate the mean crystal size from the Debye-Scherrer equation.

Thickness was measured by mechanical profilometry on a Dektak stylus (Veeco).

Dye loading determination was performed following Neale procedure[22]. The films are soaked in a N719 (Solaronix) ethanolic solution during 5 h, then desorbed in KOH 1 mM. The absorbance of the resulting solution is measured on a UV-vis spectrometer (Perkin Elmer Lambda14P). Dye loading is calculated by using a calibration curve and accurately measuring the surface of the film.

## 3. Results and Discussion

All films were submitted to several microstructural characterizations in order to investigate film thickness, size and distribution of pores, crystallization and crystal size, and finally dye loading. The data are summarized in table 1.

The soft-templating procedure reported by Malfatti et al.[8] produces very thin films, on the order of only 30 nm per layer, which is far too low for the targeted applications. We increased the solution concentration and dip-coating speed to prepare thin films with ~140 nm thickness. A six-layer film of 850 nm was obtained by repeating the sequence dipping-stabilization six times, followed by a final thermal treatment for calcination (ST sample). The films are homogeneous and crack-free.

We used the spin-coating deposition technique to prepare dual templated films (DT samples) containing P123 and PS nanospheres as structuring agents. This technique necessitates less solution and gives thicker films up to one micron, depending on the viscosity and rotation speed. The DT films show a regular and crack-free surface after one spin-coating cycle, but need further improvement for multi-layer coating.

### 3.1 Porosity

We checked the presence of porosity by TEM. This microscopy technique is well suited for such bimodal range of pores, which can be evidenced by combining medium magnification and high magnification images. On the contrary, methods based on gas adsorption such as nitrogen in BET or water in poroellipsometry are limited to mesopores with a maximum diameter of a few tens of nanometers.

Figure 2 shows TEM micrographs of ST sample, highlighting the coexistence of macropores and small, well-defined mesopores. As expected, the addition of PPG influences the size of mesopores at two different length scales. The mean diameter of both populations of pores show distributions centered around 54 nm and 10 nm. The smallest pores correspond to the F127 templating. It is worth noting that the pore size has slightly increased when compared to a F127/Ti system without PPG, which usually leads to mesoporous $TiO_2$ structure with pores around 7-8 nm[23].This indicates partial solubilization of the swelling agent PPG in the core of the F127 micelles, constituted by the polypropylene oxide block. Addition of PPG to this system not only leads to an increase in the size of the small mesopores, but also gives rise to a distinct population of large pores, attributed to a macroscopic phase separation process during

the evaporation of the solvent out of the film. The large pores are the imprints of this demixing PPG-rich phase.

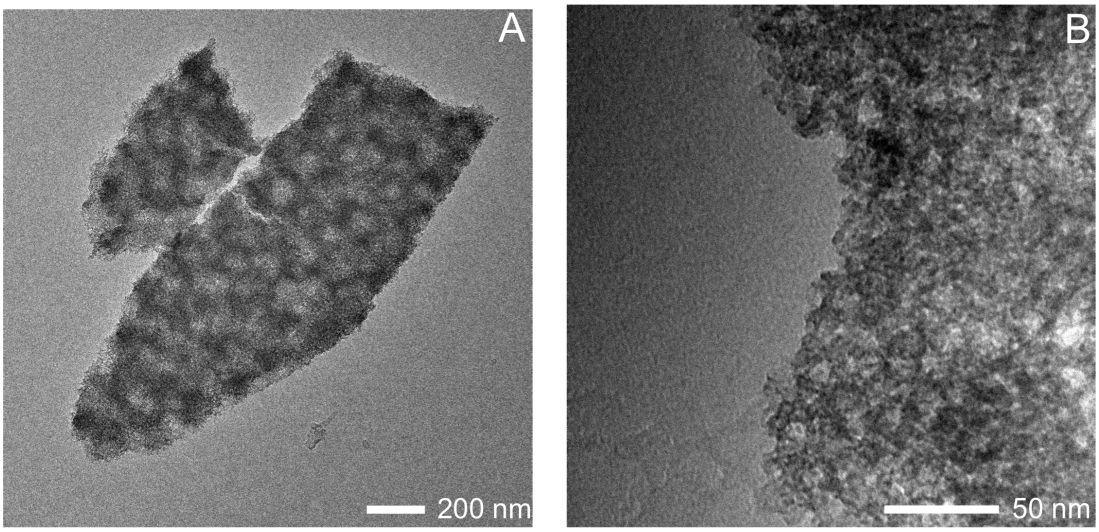


**Figure 2.** ***TEM Micrographs of ST (F127+PPG) after calcination at 350°C during 2h. A) medium magnification, showing large pores with diameter of 54 nm. B) high magnification showing spherical mesopores with diameter of 10 nm***

We observed DT-250 sample by SEM and TEM. The removal of PS nanospheres by calcination leads to pores with a diameter 20-30% smaller than the original beads size, as already reported in references [16,20]. After calcination, $TiO_2$ forms an interconnected, hexagonal network adopting the 3D organization of the PS nanospheres (Figure 3). The thickness of the walls is estimated to be around 42 nm, while the diameter of pores varies from 165 nm to 200 nm, depending on the observed area (surface vs. depth) and imaging technique (SEM vs. TEM, Figure 3 and Figure 4, A).

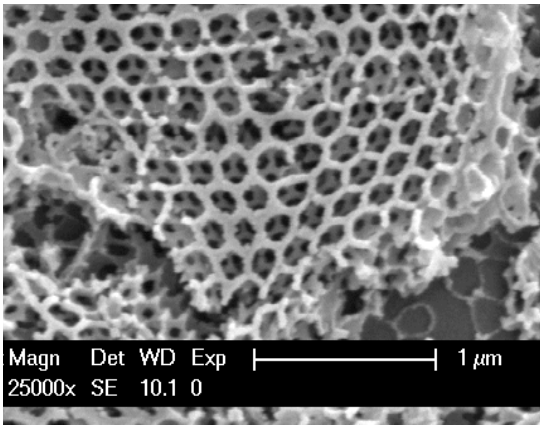


**Figure 3: SEM micrograph of DT-250 sample showing the hexagonal, interconnected network of $TiO_2$ walls after calcination.**

The walls surrounding the macropores are composed by a random stacking of tiny Anatase particles, constituting an assembly typically obtained shortly after the collapsing of a soft-templated mesoporous structure (Figure 4, B). We determined the particle size from the X-ray diffraction patterns (see below) to be 11 nm. While it does not show any spherical mesopores anymore, this random close packing of small particles gives rise to a highly mesoporous network with pore size around 6-8 nm and percentage of air on the order of 38%. These values were determined by poro-ellipsometry with water as an adsorbent, on soft-templated films P123/Ti heat treated in the same conditions (results not shown here[23]).

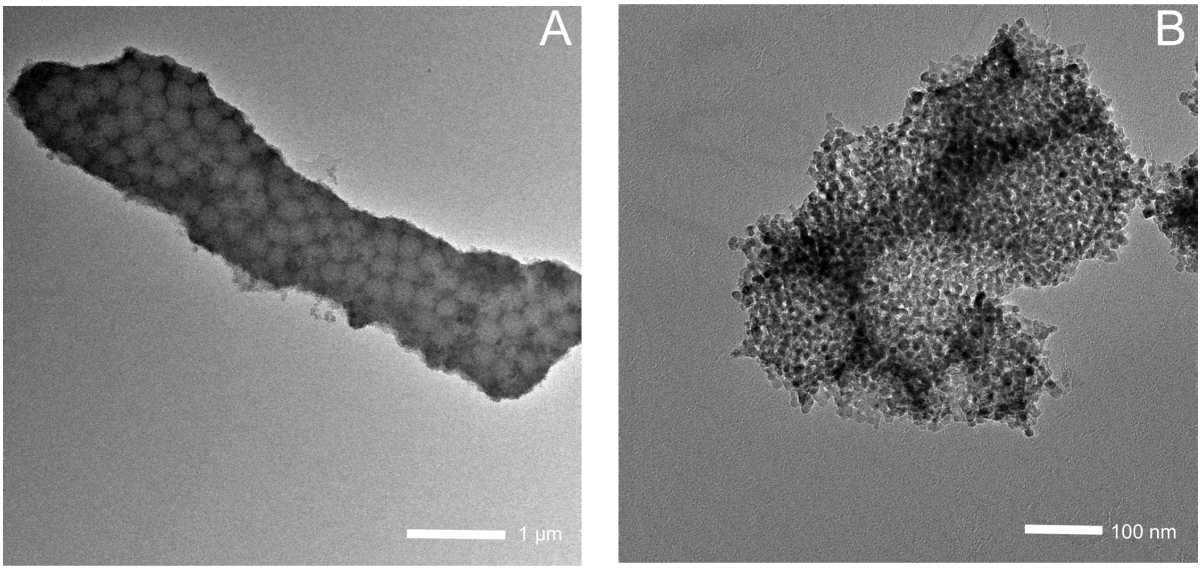


**Figure 4 : TEM Micrographs of DT-250 after calcination at 360°C A) medium magnification, showing large pores with diameter 165-200 nm. B) high magnification showing mesoporous stacking of small particles (diam. 11 nm).**

### 3.2 Tuning of thermal treatment.

The thermal treatment has to be finely tuned in order to completely remove the organic templates (micelles and nanospheres if present), eliminate by-products and induce the crystallization of the Anatase phase. Insufficient calcination produces amorphous films with poor photoelectronic properties or carbon residues. Overheating of the film leads to a decrease of specific surface due to excessive grain growth and sintering, which is deleterious for dye adsorption or photocatalysis process. Additionnaly, the presence of organic material in the film as well as the duration and temperature of the stabilization step generally influence the crystallization process of the amorphous $TiO_2$ network[24].

ST Sample contains F127 and PPG polymers. The thermal treatment usually applied to the single template F127/Ti system consists in heating the film at 1°C/min up to 350°C and keeping the sample at this temperature for 2 hours. This thermal treatment shows to be

insufficient for the crystallization of Anatase when applied to a film containing PPG and F127 (Figure 5). We increased the temperature to 360°C and observed a well-defined Anatase peak in the XRD spectrum, indicating the crystallization of the inorganic walls. However, TEM micrograph shows that the mesoporosity has collapsed (Figure 5,A), due to excessive crystal growth. We modified the thermal treatment and tested short time exposure to 360°C. This reveals that the crystallization of Anatase has started; to a limited extend compatible with the preservation of spherical mesopores as shown by TEM (Figure 5, B). We used the Debye-Scherrer equation to extract mean crystal size from the 101 diffraction peak, which leads to 10 nm, 11 nm and 15 nm for exposure at 360°C during 10 min, 20 min and 120 min respectively. J. Dewalque reported a crystal limit size of 7.7 nm, above which the surfactant-derived spherical mesopores collapse. It appears here that the presence of PPG in the surfactant-based micelles influences the development of open porosity, along with the nucleation and crystal growth of Anatase, in such a way this threshold particle size can be overcome.

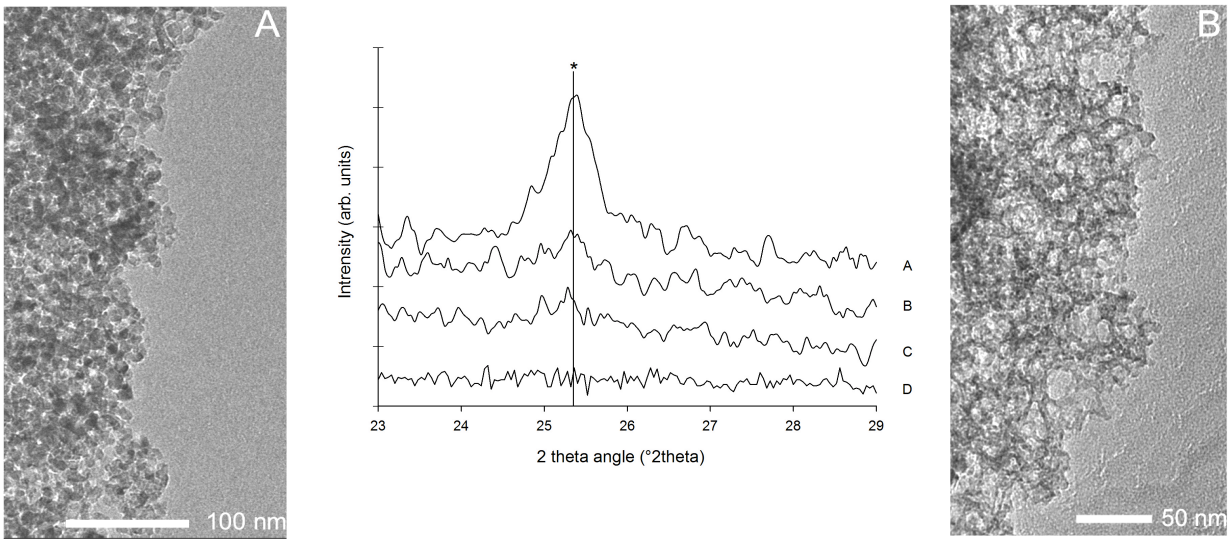


**Figure 5: Center: X-ray Diffractogramms of ST films calcined at different temperatures (heating ramp 1°C/min): A: 2h@360°C, B: 20min@360°C, C: 10min@360°C, D: 2h@350°C. Vertical line shows the position of Anatase 101 peak. Left and Right: TEM micrographs of sample ST. (A): after calcination at 360°C during 120 min, showing a collapsed structure, (B): after calcination at 360°C during 20 min, showing the spherical imprints of micelles.**

We obtained dual-templated films from a precursor solution containing both surfactant P123 and polymer nanospheres (PS 250 nm), deposited by spin coating. The thermal treatment of PS-containing films has to be adapted to insure complete removal of carbon residues. Indeed, the high thermal stability of PS leads to carbonaceous products adsorbed on the $TiO_2$ surface and weakens the sorption properties of the porous film (dye or pollutants). Therefore, DT-250 films were calcinated under oxygen flow before dye loading measurements.

XRD data recorded on DT samples show that the $TiO_2$ walls are crystallized in the form of Anatase with a mean crystallite diameter of 11 nm.

### 3.3 Dye Loading

We estimated the surface area available for dye adsorption based on simple geometrical models. We compared the calculated values with the experimental covering by N719 dye molecules, thereby checking the accessibility of pores towards the infiltration of large molecules.

For single template films, the model relays on the Random Close Packing (RCP) of spheres, normally giving 64% of spheres and 36% of void. However, this model can be slightly modified by using the actual percentage of air determined by ellipsometry. The specific surface of RCP arrangement of particles is given by equation 1:

$$Ss = \frac{(\%solid).3}{r} \qquad \text{equation 1}$$

With r = radius of spherical particles and %solid = 1- % air.

For example, a surfactant-templated film (without any swelling agent), treated for 30 min at 500°C, gives rise to a stacking of particles with diameter 10 nm and 39.5% of porosity. The calculated specific surface would be:

$$Ss = \frac{(1-0.395).3}{5\,10^{-9}} = 3.63\,10^{8}\,m^2/m^3$$

For a hierarchically porous film like DT-250 showing large pores arranged in a hexagonal non compact structure, separated by thick walls of nanoparticles in RCP, we use the following equations:

$$V_{macropores} = 0.74\left(\frac{r}{r+\Delta}\right)^3$$ equation 2

Where r = macropores radius and 2Δ = wall thickness

$$V_{walls} = 1 - V_{macropores}$$ equation 3

$$Ss_{macro} = \frac{V_{macropores}.3}{r}$$ equation 4

$$Ss_{meso} = V_{walls}.Ss_{pluronic}$$ equation 5

Where $Ss_{pluronic}$ is the corresponding Ss of pure surfactant-templated film without hard template

$$S_{N719} = DL.N_A.10^{12}.A_{N719}$$ equation 6

Where DL is Dye Loading, $N_A$ is Avogadro number, $A_{N719}$ is the surface occupied by a single N719 molecule = 2.43 $10^{-18}$m$^2$ ( 0.41 molecule/ nm$^2$)[22].

ST sample is constituted by nanoparticles of 11 nm and a total percentage of air around 42%. The calculated specific surface would therefore be 3.05 $10^8$ m$^2$/m$^3$ (calculated from eq. 1). The experimental determination of dye loading is 2.1 $10^{-10}$moles/(mm$^2$.µm) of N719, which corresponds to a surface coverage of 3.1 $10^8$ m$^2$/m$^3$ (calculated from eq. 6) . This very good agreement between experimental and calculated values proves the total accessibility of bimodal porosity towards dye adsorption, reported to be limited to pores larger than 4 nm[25].

The modeling of DT-250 films is based on a porous structure with a combination of macropores and mesoporous walls.

The macropores occupy a volume proportion of 0.474 (calculated from eq.2), while the mesoporous thick walls occupy 0.536 of the total volume. In the walls, there is an additional proportion of air induced by mesopores that constitutes 39.5% of the walls themselves, which gives 0.536 x 0.395=0.208. The total percentage of air in DT-250 is therefore estimated to be 0.474+0.208= 0.682 = 68%. Experimentally, we found a percentage of air of 65% in DT-250 film, determined by ellipsometry, which is in good agreement with the calculated value and indicates that both templates (Pluronic and PS beads) have been totally removed.

The specific surface associated to this bimodal porosity can be calculated in the same way, considering the surface of macropores ($Ss_{macro}$) and the specific surface inside mesoporous walls ( $Ss_{meso}$). According to equations 1, 4 and 5, the contributions to specific surface can be evaluated to be $Ss_{macro} = 1.40\ \ 10^7\ m^2/m^3$ and $Ss_{meso} = 2.23\ \ 10^8\ m^2/m^3$, giving a $Ss_{total} = 2.37\ 10^8\ m^2/m^3$.

The dye loading of DT-250 has been measured to be $1.7\ \ 10^{-10}$ mol/($mm^2$.µm), which gives an occupied surface of $2.4\ \ 10^8\ m^2/m^3$, again in excellent agreement with the calculated value.

As a comparison, pure Pluronic-templated films (P123 alone) give a dye loading of $2.9\ \ 10^{-10}$mol/($mm^2$.µm) when treated in similar conditions. Not surprisingly, the introduction of larger pores in the mesoporous structure results in a decrease of total specific surface area. The larger the pores, the lower the specific surface. However, combining mesoporosity produced by the soft-templating system within the walls and larger pores allows maintaining very high values of Ss with an optimum access for the infiltration of large species. As an example, in DSSC technology, the commercially available porous anatase photoanodes are prepared by printing techniques from nanoparticulate pastes. They are composed of particles with diameter of 20 nm, which gives a calculated Ss of $1.92\ \ 10^8 m^2/m^3$ and hardly gives an experimental value of $1.6\ \ 10^8 m^2/m^3$, determined by N719 dye loading. This type of porous

film are not only limited in terms of overall adsorption capability (due to large particle size) but also present a narrow porous network unsuitable for the infiltration of solid state electrolyte, widely studied in an attempt to get rid of liquid component in PV cells[26-29].

## 4. Conclusions

We have prepared hierarchically porous thin films by two experimental routes based on soft-templating and dual templating. Both techniques are derived from the classical Pluronic-templated synthesis of mesoporous Anatase films. The objective is to introduce a second population of pores to facilitate the accessibility of large species while keeping very high values of specific surface. The target is a combination of nanocrystalline Anatase and open porosity.

The ST route relies on the swelling of existing Pluronic micelles by PPG, which results in the demixing of large, PPG-rich micelles. The pore sizes are 10 nm and 54 nm. The films keep a high specific surface, equivalent to 71% of the corresponding pure-Pluronic template films.

The DT route uses PS nanospheres as a second template, which does not interfere with the Pluronic-$TiO_2$ system. When using PS beads of 250 nm, the bimodal porous structure shows pore sizes of 8 nm and 165-200 nm after calcination. The specific surface is still 57% of a pure-Pluronic template film.

The specific surface of hierarchically porous films is still much higher than commercially available porous photoanodes, whose porosity is only 37% compared to a Pluronic-templated

film. Furthermore, their porous network is not suitable for the infiltration of large species like viscous polymers, restraining their field of applications to gas or liquid-based interfaces.

The one-pot dual templating presented here gives nice pores monodispersity, promising high selectivity in catalysis applications. The procedure described is time saving as compared to others. The hard templates are available in a large range of diameter. The simple geometrical model presented here can be used to predict the specific surface and percentage of pores in the bimodal porous structures obtained. Furthermore, it can be easily extended to other sol-gel materials and the resulting hierarchical porous structures are therefore of wide interest in porous materials science.

## 5. Acknowledgment

*Prof. B. Heinrichs is acknowledged for access to profilometry measurements. J. Jonlet acknowledges IDS FunMAT ( International Doctorate School in Functional Materials) for a PhD fellowship.*

## 6. References


[1] M. Gratzel, Nature 414 (2001) 338.

[2] L. Andronic, D. Andrasi, A. Enesca, M. Visa, A. Duta, J Sol-Gel Sci Technol 58 (2010) 201.

[3] G. Yang, P. Hu, Y. Cao, F. Yuan, R. Xu, Nanoscale Res Lett 5 (2010) 1437.

[4] S.U.M. Khan, Science 297 (2002) 2243.

[5] Z.-Y. Yuan, B.-L. Su, J. Mater. Chem. 16 (2006) 663.

[6] D. Grosso, A.R. Balkenende, P.A. Albouy, A. Ayral, H. Amenitsch, F. Babonneau, Chem. Mater. 13 (2001) 1848.

[7] C.J. Brinker, Y. Lu, A. Sellinger, Adv. Mater. 11 (1999) 579.

[8] L. Malfatti, M.G. Bellino, P. Innocenzi, G.J.A.A. Soler-Illia, Chem. Mater. 21 (2009) 2763.

[9] Y. Hu, K. Qian, P. Yuan, Y. Wang, C. Yu, Mat. Lett. 65 (2011) 21.

[10] M. Kruk, Acc. Chem. Res. 45 (2012) 1678

[11] O.D. Velev, T.A. Jede, R.F. Lobo, A.M. Lenhoff, Nature 389 (1997) 447.

[12] B.T. Holland, Science 281 (1998) 538.

[13] S.H. Park, Y. Xia, Chem. Mater. 10 (1998) 1745.

[14] D. Wang, R.A. Caruso, F. Caruso, Chem. Mater. 13 (2001) 364.

[15] M. Jin, S.S. Kim, M. Yoon, Z. Li, Y.Y. Lee, J.M. Kim, J. Nanosci. Nanotech. 12 (2012) 815.

[16] J. Zhao, P. Wan, J. Xiang, T. Tong, L. Dong, Z. Gao, X. Shen, H. Tong, Micropor. Mesopor. Mat. 138 (2011) 200.

[17] T. Sen, G.J.T. Tiddy, J.L. Casci, M.W. Anderson, Chem. Mater. 16 (2004) 2044.

[18] C.G. Oh, Y. Baek, S.K. Ihm, Adv. Mater. 17 (2005) 270.

[19] P. Yang, Science 282 (1998) 2244.

[20] L. Qi, D.P. Birnie III, Mater. Lett. 61 (2007) 2191.

[21] D.A.G. Bruggeman, Ann. Phys. (Berlin, Ger.) 24 (n.d.) 636.

[22] N.R. Neale, N. Kopidakis, J. van de Lagemaat, M. Grätzel, A.J. Frank, J. Phys. Chem. B 109 (2005) 23183.

[23] J. Dewalque, R. Cloots, F. Mathis, O. Dubreuil, N. Krins, C. Henrist, J. Mater. Chem. 21 (2011) 7356.

[24] J. Dewalque, R. Cloots, O. Dubreuil, N. Krins, B. Vertruyen, C. Henrist, Thin Solid Films 520 (2012) 5272.

[25] K.-J. Hwang, W.-G. Shim, S.-H. Jung, S.-J. Yoo, J.-W. Lee, Applied Surf. Sci. 256 (2010) 5428.

[26] I.K. Ding, J. Melas-Kyriazi, N.-L. Cevey-Ha, K.G. Chittibabu, S.M. Zakeeruddin, M. Graetzel, M. D. McGehee, Org. Electron. 11/7 (2010), 1217.

[27] I.K. Ding, N.Tetreault, J. Brillet, B.E. Hardin, E.H. Smith, S.J. Rosenthal, F. Sauvage, M. Graetzel, M.D. McGehee, Adv. Funct. Mater. 19/15 (2009) 2431.

[28] H.J. Snaith, R. Humphry-Baker, P. Chen, I. Cesar, S.M. Zakeeruddin, M. Gratzel, Nanotechnology 19/42 (2008) 424003/1.

[29] J. Melas-Kyriazi, I.-K Ding, A. Marchioro, A. Punzi, B.E. Hardin,G.F. Burkhard, N. Tetreault, M. Gratzel,J.-E. Moser, M.D. McGehee, Adv. Energy Mater. 1/3 (2011) 407.

## 7. Figures Captions

Figure 1: Flowchart of dual templating route. TTIP stands for Ti isopropoxide

Figure 2: TEM Micrographs of ST (F127+PPG) after calcination at 350°C during 2h. A) medium magnification, showing large pores with diameter 54 nm. B) high magnification showing spherical mesopores with diameter 10 nm

Figure 3: SEM micrograph of sample DT-250 showing the hexagonal, interconnected network of $TiO_2$ walls after calcination.

Figure 4: TEM Micrographs of DT-250 after calcination at 360°C A) medium magnification, showing large pores with diameter 165-200 nm. B) high magnification showing mesoporous stacking of small particles (diam. 11 nm).

Figure 5: Center: X-ray diffraction patterns of ST films calcined at different temperatures (heating ramp 1°C/min): A: 2h@360°C, B: 20min@360°C, C: 10min@360°C, D: 2h@350°C. Vertical line shows the position of anatase 101 peak. Left and Right: TEM micrographs of sample ST. (A): after calcination at 360°C during 120 min, showing a collapsed structure, (B): after calcination at 360°C during 20 min, showing the spherical imprints of micelles.

## 8. Tables Captions

Table I: Summary of synthesis details and data from structural characterization.

*dye loading values are normalized to a thickness of 1.00 µm

| Sample code | Templates | Deposition | Thermal treatment | Thickn./ nm | Pores sizes/nm (bimodal) | | Grain size nm | % air | Dye Loading* mol/mm$^2$.1µm |
|---|---|---|---|---|---|---|---|---|---|
| ST | F127 + PPG | Dip-coating ( 6 layers) | 60°C/h 360°C 20 min | 854 | 10 | 54 | 11 | 42 | 2.06 $10^{e-10}$ |
| DT-250 | P123 + PS 250 | Spin-coating | 500°C/h 500°C 30 min | 1081 | (6 -8) | (165 -200) | 11 | 65 | 1.65 $10^{e-10}$ |